Predatory posture and performance in a precocious larval fish targeting evasive copepods

Mary C. Fashingbauer[1], Lillian J. Tuttle[1]*, H. Eve Robinson[1,2], J. Rudi Strickler[3,4], Daniel K. Hartline[1], Petra H. Lenz[1]

[1] Pacific Biosciences Research Center, Honolulu, HI 96822, USA

[2] Department of Biological Sciences, Humboldt State University, Arcata, CA 95521, USA

[3] Department of Biological Sciences, University of Wisconsin-Milwaukee, Milwaukee, WI 53204, USA

[4] Marine Science Institute, University of Texas at Austin, Port Aransas, TX 78373, USA

*Corresponding author: tuttlel@hawaii.edu

Key Words: fast-start, predation, evasive prey, S-start, kinematics

Summary Statement

We investigate a highly modified and previously undescribed fast-start of a larval coral-reef fish, which as early as one day after hatching, captures evasive copepod prey.

Abstract

Predatory fishes avoid detection by prey through a stealthy approach, followed by a rapid and precise fast-start strike. While many first-feeding fish larvae strike at non-evasive prey using an S-start, the clownfish *Amphiprion ocellaris* feeds on highly evasive calanoid copepods from a J-shaped position, beginning 1 day post-hatch (dph). We quantified this unique strike posture by observing successful predatory interactions between larval clownfish (1 to 14 dph) and three developmental stages of the calanoid copepod *Bestiolina similis*. The J-shaped posture of clownfish became less tightly curled (more L-shaped) during larval development. Larvae were also less tightly curled when targeting adult copepods, which are more evasive than younger copepod stages. Strike performance, measured as time-to-capture and peak speed, improved only slightly with larval age. Therefore, the J-posture may allow first-feeding larvae to minimize disturbance during their approach of sensitive prey, and may represent an alternative predatory strategy to the prototypical S-start.

Introduction

Fast-starts in fishes, the rapid acceleration from a near motionless state to one of high speed, are either C-starts or S-starts, where the former is used in escape reactions and the latter in predatory strikes (Domenici and Blake, 1997; Harper and Blake, 1991; Webb and Skadsen, 1980). In setting up for a predatory strike, the fish bends into an "S" shape with its head and caudal fin pointing in opposite directions, then rapidly straightens its body toward the prey (Domenici and Blake, 1997; Harper and Blake, 1991). Predatory strikes with S-starts are best described in juvenile and adult fishes, but they have also been documented for some larval fishes, including herring, anchovy, and zebrafish (Fig. 1S; Borla et al., 2012; Hunter, 1972; McClenahan et al., 2012; Rosenthal, 1969), which have served as the basis for our understanding of feeding in larval fish. However, it is unlikely that all larval fishes use S-starts to strike at their prey. Leis and Carson-Ewart (1998) presented the first *in situ* observations of pelagic larvae of coral-reef fishes and noted that "the classic 'S' or 'C' pre-strike posture…was not evident" in 30

observations of 21 species from nine families. Their study did not include a description of the strike posture other than stating that larvae used "feeding behaviours similar to those of adults."

During fish larvae's transition to exogenous feeding ("first-feeding"), S-starts can lack precision and have maximum speeds below 100 mm s^{-1} with time to capture >10 ms (China et al., 2017; Hunter, 1972; McClenahan et al., 2012; Rosenthal, 1969; Rosenthal and Hempel, 1970). As a result, some first-feeding larvae have difficulty capturing evasive prey and target non-evasive prey instead. For example, larval cod (*Gadus morhua*) prefer non-evasive protozoa until four to five days after first-feeding (9 days post-hatch, dph), at which time they begin to target early stages of evasive copepods (von Herbing and Gallager, 2000). However, many other first-feeding larvae successfully capture calanoid copepods as demonstrated in both laboratory studies (Jackson and Lenz, 2016; Robinson et al., 2019) and gut-content analyses of wild-caught larvae (Llopiz and Cowen, 2009; Østergaard et al., 2005). What is the fast-start posture of these precocious fish larvae and does it differ from larval fish that target non-evasive prey?

Our goal was to resolve the apparent paradox between the expected fast-start (S-start) predatory strike and the observed feeding behaviour of some fish larvae (e.g., Leis and Carson-Ewart, 1998). Here, we describe the pre-strike posture and changes in body form during the strike of a first-feeding fish that captures evasive copepods and assess if its strike posture changes during ontogeny. Additionally, we varied the developmental stage of the copepod prey to determine whether larval predators adjust their feeding behaviour accordingly. In so doing, we characterize a previously undescribed posture that a stealthy larval fish assumes before initiating a rapid and accurate strike toward its prey.

Materials and methods

Our experimental design set three larval fish age-classes of the clownfish, *Amphiprion ocellaris* (early: 1 to 5 days post-hatch [dph]; mid: 6 to 9 dph; and late: 11 to 14 dph) against three developmental stages of the copepod prey, *Bestiolina similis* (nauplii: NIII-NIV stages; copepodites: CII-CIII stages; and adults: CVI stage). The choice of developmental stages provided a range in prey size (length: ~100 to 500 µm; McKinnon et al., 2003), mechanosensitivity, and escape performance (Bradley et al., 2013; Buskey et al., 2017). We designed the experiment to quantify how strike posture changed through larval development (size: ~4 to 8 mm total length; Jackson and Lenz, 2016), while also assessing the effect of a

prey's stage on its predator's posture. Animal husbandry and experimental protocols followed institutional guidelines and were approved by the University of Hawai'i Institutional Animal Care & Use Committee (IACUC protocol number 2099).

Larval fish-rearing conditions

The experiments used larval clownfish lab-reared over their two-week planktonic phase. The rearing of fish, the culturing of copepod prey, the experimental apparatus and protocols, and the high-speed video recording and analysis software have been described previously (Robinson et al., 2019). Briefly, up to 200 recently hatched larvae were raised in a 30-L seawater aquarium kept at 24-26° C on a 12:12 L:D light cycle. They were fed twice daily on a mixed diet of rotifers (*Brachionus plicatilis*) and different developmental stages of another calanoid copepod (*Parvocalanus crassirostris*). Different prey were used for daily feeding than for experiments so that fish were exposed to a novel prey type during their trial, thus avoiding complications arising from learned feeding behaviour and laboratory acclimation.

Behavioural observations and video set-up

For the experiments, two larvae that had been kept without food for 4 to 6 hours were placed into a circular observation chamber of 20 cm diameter, filled with seawater to a depth of 2 cm containing copepods at a density of 0.2 to 0.7 individuals ml^{-1}. Experimental trials lasted for one hour or less and no fish larvae were used in more than one trial. Interactions between fish larvae and copepods were recorded at 500 frames per second (fps) using a Photron FastCAM SA4 video camera mounted above the observation chamber with dark-field illumination. The field-of-view of the camera was 35 x 35 mm with an image resolution of 1024 x 1024 pixels. To produce Fig. 1, we used Adobe Photoshop to make the following adjustments to each image: we inverted black and white, applied a level with settings 200/0.8/245, and cropped to the same scale across time and fish age. For ease of visual comparison, we also rotated and flipped each image such that the fish faced up with its tail bent to the right (originally bent to left: n=18; to right: n=19). We did not add to, alter, enhance, obscure, move, or remove any specific feature of an image.

Data analysis

Our goal was to quantify the final pre-strike postures of a larval fish and any changes in body form during its attack on a highly evasive prey. We analysed 37 instances in which a fish larva successfully captured a copepod by digitizing the body shape of the fish as it completed its final approach phase and thereafter its strike phase, as defined by Robinson et al. (2019). Briefly, the final approach phase began when the fish stopped beating its caudal fin and began to bend the fin to the left or right and ended at the moment just before the fish initiated its strike. The strike phase began when the fish opened its mouth, which was followed by a lunge toward the prey. Time zero (t_0) was the moment (i.e., frame) when the fish reached its final pre-strike posture just prior to opening its mouth (Longo et al., 2016), thus making t_0 a temporal reference that separated the slow final approach and the high-speed strike phases (Fig. 2S).

Twenty-five frames, including 12 frames before and 12 frames after t_0, were then extracted and the posture of the fish larva was characterized frame-by-frame. Twelve frames (24 ms) before t_0, labelled as t_{-24}, was chosen as a standardized culminating interval of the final approach phase, which ranged in total duration from 28 to 1130 ms preceding t_0. This 24-ms interval captured the final pre-strike posture (Fig. 2S, Robinson et al. 2019), which was our goal. Twelve frames after t_0, labelled as t_{+24}, was chosen as a standardized strike interval as it always included peak strike speed, copepod capture, and the initial deceleration of the fish. Starting with t_{-24} and continuing every other frame up to and including t_{+24}, we digitized the x,y coordinates of 12 points along the central axis of the larva, using the Fiji software package built on ImageJ (v1.51) (Shindelin et al., 2012). Because its position with respect to the fish did not change, we used a small pigment spot located at the narrowest point between the eyes as a spatial reference for each frame (origin at x=0, y=0). The position of the copepod in each frame was also digitized to obtain the change in distance over time between fish and copepod.

Final approach speeds were at least 2 orders of magnitude lower than strike speeds (see Fig. 2S for example), indicating that all motion involved in the acceleration of the strike occurred after t_0. Therefore, we quantified the relative curvature of the body and caudal fin during the larva's initial lunge, frame-by-frame from t_0 to t_{+8} (8 ms, i.e., 4 frames after t_0), the time interval representing the greatest change in posture (Fig. 2S). To do so, we used the oval tool in Fiji to place a circle within the curl of the tail. The "fit circle" and "measure" commands were then used

to calculate the area (A) of the circle. From the circle's area, we derived the reciprocal radius, $r^{-1} = \sqrt{(\pi / A)}$ as a metric of relative curvature of the larva's caudal fin, with greater values being more curved and lesser values being less curved (Cauchy, 1826). The measurement of reciprocal radius became less reliable as an estimate of curvature after t_{+8} because the tails of most fish began to curve in the opposing direction, making the inscribed circle too large to measure. We therefore employed another relative measure of curvature, the straight-line distance between the tip of the tail and the narrowest point between the eyes (chord length), divided by the length of the fish when its body was straight (fish length), also measured between the tip of the tail and origin/pigment. These normalized distances (chord length-to-fish length ratio, or CVF) approached 1 when the fish was straight and were decreasing fractions of 1 when the fish was increasingly bent into a J-like posture. To measure speed of the fish during its predatory lunge (in mm s^{-1}), we tracked the changing position of the pigment between its eyes from t_{-4} to t_{+20} (4 ms, i.e., 2 frames before t_0 and 20 ms, i.e., 10 frames after t_0, respectively) and divided the frame-by-frame distance travelled by the time elapsed between frames. In addition, the distance from the spot between the eyes and the tip of the mouth was measured at t_0 and t_{+8} to determine the contribution of jaw extension to prey capture.

All statistical tests were conducted in R software v3.4.1 (R Core Team, 2017). To compare curvature in terms of CVF, a continuous and proportional index with inherent heteroskedasticity, we used beta regression (R package *betareg*, v3.2) as set forth by Cribari-Neto and Zeileis (2010). To determine whether the fish's body curvature changed in response to both its age and targeted prey type, we fitted the following model: CVF ~ prey-stage + fish age in dph + interaction between prey-stage and fish age (Table S1). We conducted a similar analysis within the late age-class of fish (11-14 dph), but without the interaction term due to the relatively small sample size (n=12) of this data subset (Table S1). We also used multiple linear regression to model how the log of peak strike speed was affected by distance between fish and copepod at t_0 (i.e., "strike distance"), fish age-class, and prey-stage (Table S1). We assessed assumptions of regression models using residual plots. For comparisons of responses by fish age-class only, we used the non-parametric Wilcoxon rank-sum test, with pairwise p-values corrected using the Benjamini-Hochberg method for multiple comparisons. The original images and dataset from which these analyses were based are publicly available at BCO-DMO (Lenz and Hartline, 2018).

Results and Discussion

Similar to S-starts, the predatory fast-start of clownfish larvae (*Amphiprion ocellaris*) had three phases: the final approach phase that culminated in setting up the strike posture, the propulsive stroke or strike, and the return to swimming (Robinson et al. 2019). At 394±38 ms prior to the strike (mean±SEM; range: 28 to 1130 ms), the larval fish stopped beating its caudal fin and started flexing its body into the strike posture while slowly positioning itself closer to the prey, at a distance of 0.9±0.1 mm at t_0 (mean±SEM; range: 0.3 to 2.1 mm). During the strike, the larva propelled itself with a rapid extension of its tail from a J-shaped, or "fish hook," posture (Fig. 1, Movie S1). After the strike, it resumed normal forward swimming. To describe the predatory posture of a precocious larval fish, we quantify only those final approaches and rapid strikes that led to capture without alerting the copepod prey, *Bestiolina similis*.

At 24 ms before the strike (t_{-24}), the larva was already close to the prey and approaching the final strike posture, as shown in Figure 1 using examples from three different age-classes of larvae. During their final approach, the two younger larvae made slight adjustments to the curl in their caudal fins (Fig. 1B,D), but this movement was minimal compared with that of the older larva, which continued to bend its tail into its final posture (Fig. 1F). Between t_{-24} and t_0, larval swimming was limited to sculling slowly with alternating strokes of the pectoral fins. Over this 24-ms time interval, the median distance moved (measured as the change in the x,y coordinates of spot between the eyes) was 69 µm (interquartile range: 35 to 77 µm), small in comparison with the distance to the copepod at t_0. The copepod remained immobile up to the strike and often through capture. In the final strike posture at t_0, the fish's body had two flexures in opposing directions, which were more evident in early- and mid-stage larvae (0 ms; Fig. 1A,C) than in late-stage larva (0 ms, Fig. 1E). While double flexure is also characteristic of the S-start posture, what is unusual about the clownfish is the extreme hook-like bend with the tail pointing either forward or perpendicular to the orientation of the fish. In contrast, the head and tail point in opposite directions in the S-start postures of larval herring and anchovy (Hunter, 1972; Rosenthal, 1969).

The movement of the pectoral fins during the final approach by the clownfish differed from that described in other fish larvae. Setting up for the S-shape, anchovy larvae continue propelling themselves with tail-beats while their pectoral fins primarily stabilize and steer

(Hunter, 1972). Re-orientation of those larvae can occur just prior to the strike, in response to movement by the prey (ca. 500 µm in Fig. 5 in Hunter, 1972). Thus, the pectoral fins are involved in stabilization so as to prevent counter-rotation or backward creep during a tail-bend, as well as assistance with J-turns, which reorient the fish towards the prey during its initial approach as shown in detail in zebrafish (McClenahan et al., 2012). During the zebrafish's predatory approach, their pectoral fins moved in and out of phase at slow swim speeds <25 mm s^{-1} (ca. <5 BL s^{-1} in Fig. 6 in McClenahan et al., 2012) with pectoral fin beat frequency of ca. 20 Hz. Clownfish, which target immobile but highly mechanosensitive prey, maintain a stable orientation. Their pectoral fins beat 180º out-of-phase during the slow approach, which is similar to the alternating pattern described in slowly swimming (<4 BL s^{-1}) juvenile reef fishes with pectoral fin beat frequencies of ca. 15 Hz (Hale et al., 2006). In clownfish larvae, this swim gait is already present at 1-dph, suggesting that it is an important component of the predatory fast-start in this species.

Larval fish in the various age-classes in our experiments avoided certain developmental stages of prey (Fig. 2). Only the mid-stage fish larvae attacked all three stages. The youngest larvae attacked nauplii and copepodites, while the oldest larvae preyed on copepodites and adults. Accompanying these changes, the strike posture at the moment preceding the attack, t_0, changed with both larval age-class and prey-stage (Fig. 2). At t_0, the bodies of early-stage larvae were consistently in a J-shaped, "fish hook" posture (Fig. 2A,B). In contrast, late-stage larvae usually executed an L-shaped, "hockey stick" posture, especially when targeting adult copepods (Fig. 2G). Fish that attacked adult copepods were significantly less tightly curled (had greater CVF) than those that attacked either copepodites (beta regression [βreg]: P=0.03) or nauplii (P=0.02), after accounting for fish age (Table S1).

Ontogenetic changes in attack strategy are likely due, at least in part, to the larvae's neurodevelopment. *A. ocellaris* has fully functional musculoskeletal linkages of their feeding apparatus and ossification of their neurocranium by 7 dph (Wittenrich and Turingan, 2011). We thus made comparisons within the late-stage larval group (11-14 dph, n=12), which allowed us to assess how prey-stage affected strike posture in these well-developed larvae. Prey-stage and larval age jointly affected the curvature (CVF) of late-stage larvae at t_0. Late-stage larvae that targeted adult copepods were 87% less curved (had greater CVF) than those that targeted copepodites (95% CI 23-184%, βreg: P=0.003; Table S1). Concurrently, for each day between

11 and 14 dph, the curvature of the fish's body at t_0 decreased by 36% (95% CI 0.4-83%, βreg: P=0.05; Table S1).

During the strike, forward movement was produced with the rapid extension of the tail (Fig. 1; 0 to 24 ms). From fully bent at t_0, the tail remained slightly bent at t_{+4} but had straightened by t_{+8} when the prey was captured (Fig. 1A,C,E). The strikes, which were directed at the prey, were either straight ahead along the line of the final approach-orientation, or slightly offset (Robinson et al., 2019). Strike distances (distance between fish and copepod at t_0) were typically less than 1 mm and were significantly smaller for early-stage larvae preying on nauplii and copepodites than for late-stage larvae preying on copepodites and adults (mean=0.7 vs. 1.0 mm; pairwise Wilcoxon rank-sum test [RS]: P=0.03). The larval strike included both body and jaw ram to minimize time-to-capture (from t_0). Jaw extension, measured between t_0 and t_{+8}, increased from ca. 0.25 to 0.5 mm between the early- and late-stage larvae. This corresponded to an increasing contribution of jaw ram to the forward lunge from 40% for early-stage larvae to 60% for late-stage larvae.

The predatory strike was limited to a single tail-beat cycle, which is similar to the Type I S-start described by Harper and Blake (1991). In the early- and mid-stage larvae, the uncurling of the tail was followed by a tail beat in the opposite direction (Fig. 1A-D). In the late-stage clownfish larvae, however, the tail straightened during the lunge (Fig. 1E,F) as shown quantitatively in the time-course of change in body shape during the strike (Fig. 3). During the strike, the body straightened very quickly, becoming nearly linear by t_{+8} in all predator-prey categories (CVF between 0.9 and 1, Fig. 3B). Thereafter, the body remained relatively straight in the older larvae, while in the younger larvae CVF decreased as the body undulated through a full tail-beat cycle (Fig. 3B).

Measurements of strike performance included time-to-capture (from t_0) and peak strike speed during the strike. Between early- and late-stage larvae, mean time-to-capture decreased from 9 to 7 ms (RS: P=0.03). Mean peak speed increased from 160 to 240 mm s^{-1} between early- and late-stage larvae, but this change was not significant (multiple linear regression [MLR]: P>0.1) after accounting for strike distance and prey-stage (Fig. 3C, Table S1). A 1-mm increase in strike distance corresponded with a 64% increase in peak strike speed (Fig. 3C; 95% CI 27-112%, MLR: P<0.001; Table S1). Concurrently, peak strike speeds of larvae on copepodites and adult copepods were 35% (95% CI 10-67%; MLR: P=0.006) and 34% (95% CI 3-74%; MLR:

P=0.03) greater than those on nauplii, respectively (Table S1, see also Robinson et al., 2019). While there was evidence of improved performance in older larvae, these changes were modest in comparison with the large increases in size and development of the jaw, gape size, and digestive and feeding systems (Green and McCormick, 2001; Jackson and Lenz, 2016; Wittenrich and Turingan, 2011). Ontogenetic overlap in strike performance suggests that larval clownfish are competent predators at first-feeding, in contrast with many other larval fishes.

To be successful hunters, larval fishes must first locate a prey and then use optimal kinematics to approach and capture it (Voesenek et al. 2018). Which strategy is "optimal" depends on the prey's behaviour, especially its ability to detect and escape from the predator (Tuttle et al. 2019). Our current understanding of larval feeding kinematics is limited to fish that use S-starts to target non-evasive prey (review: Voesenek et al., 2018), which is distinct from the highly modified and previously unrecognized fast-start described for the clownfish. The combination of the clownfish's extreme J-shaped posture and alternate sculling of its pectoral fins likely minimizes disturbance during its predatory approach while precisely aligning it with the prey. While early fish larvae are similar morphologically, clownfishes are precocious in their development and predatory prowess when compared with others (Green and McCormick, 2001; Kavanagh and Alford, 2003; Wittenrich and Turingan, 2011; Kavanagh and Frédérich, 2016). Furthermore, diets of larval fishes are diverse, and specialized diets likely require different predatory strategies. Thus, the modified strike posture of the clownfish may be just one example of an alternate fast-start that has evolved in larval fishes. Future studies should explore the relationship between prey behaviour and predatory strategies of larval fishes during their first, critical stage of life.

Acknowledgements

We thank T. Cabalar, B. Coffey, Y. Niimi and J. Suitos for their assistance with culturing and larval rearing, and Karen Brittain for providing clownfish eggs and rotifers. This is SOEST contribution number ####.

Financial Support

Financial support was provided by the National Science Foundation (OCE 12-35549 to PHL and DKH). The views expressed herein are those of the authors and do not reflect the views of NSF or any of its sub-agencies.

References

Borla, M. A., Palecek, B., Budick, S. and O'Malley, D. M. (2012). Prey capture by larval zebrafish: evidence for fine axial motor control. *Brain, Behavior and Evolution* **60**, 207-229.

Bradley, C. J., Strickler, J. R., Buskey, E. J. and Lenz, P. H. (2013). Swimming and escape behavior in two species of calanoid copepods from nauplius to adult. *Journal of Plankton Research* **35**, 49-65.

Buskey, E. J., Strickler, J. R., Bradley, C. J., Hartline, D. K. and Lenz, P. H. (2017). Escapes in copepods: comparison between myelinate and amyelinate species. *Journal of Experimental Biology* **220**, 754-758.

Cauchy, A. L. (1826). Leçons sur les applications du calcul infinitésimal à la géomeétrie. Paris: Imprimérie Royale.

China, V., Levy, L., Liberzon, A., Elmaliach, T. and Holzman, R. (2017). Hydrodynamic regime determines the feeding success of larval fish through the modulation of strike kinematics. *Proceedings of the Royal Society B-Biological Sciences* **284**, 20170235.

Cribari-Neto, F. and Zeileis, A. (2010). Beta Regression in R. *Journal of Statistical Software* **34**, 1-24. http://www.jstatsoft.org/v34/i02/.

Domenici, P. and Blake, R. W. (1997). The kinematics and performance of fish fast-start swimming. *Journal of Experimental Biology* **200**, 1165-1178.

Green, B. S. and McCormick, M. I. (2001). Ontogeny of the digestive and feeding systems in the anemonefish *Amphiprion melanopus*. *Environmental Biology of Fishes* **61**, 73-83.

Hale, M. E., Day, R. D., Thorssen, D. H. and Westneat, M. W. (2006). Pectoral fin coordination and gait transitions in steadily swimming juvenile reef fishes. *Journal of Experimental Biology* **209**, 3708-3718.

Harper, D. G. and Blake, R. W. (1991). Prey capture and the fast-start performance of northern pike *Esox lucius. Journal of Experimental Biology* **155**, 175-192.

Hunter, J. R. (1972). Swimming and feeding behavior of larval anchovy *Engraulis mordax*. *Fishery Bulletin* **70**, 821-838.

Jackson, J. M. and Lenz, P. H. (2016). Predator-prey interactions in the plankton: larval fish feeding on evasive copepods. *Scientific Reports* **6**, 33585.

Kavanagh, K.D. and Alford, R.A. (2003). Sensory and skeletal development and growth in relation to the duration of the embryonic and larval stages in damselfishes (Pomacentridae). *Biological Journal of the Linnean Society* **80**, 187-206.

Kavanagh, K.D. and Frédérich, B. (2016). Ontogeny and Early Life Stages of Damselfishes. In *Biology of Damselfishes*, (ed. Frédérich, B. and Parmentier, E.), pp. 168-182. Boca Raton, Florida: CRC Press.

Leis, J. M. and Carson-Ewart, B. M. (1998). Complex behaviour by coral-reef fish larvae in open-water and near-reef pelagic environments. *Environmental Biology of Fishes* **53**, 259-266.

Lenz, P. H. and Hartline, D. K. (2018) Data from: High-speed videos of larval clownfish, *Amphiprion ocellaris*, predators and copepod prey. Biological and Chemical Oceanography Data Management Office (BCO-DMO). (http://lod.bco-dmo.org/id/dataset/747926)

Llopiz, J. K. and Cowen, R. K. (2009). Variability in the trophic role of coral reef fish larvae in the oceanic plankton. *Marine Ecology Progress Series* **381**, 259-272.

Longo, S. J., McGee, M. D., Oufiero, C. E., Waltzek, T. B. and Wainwright, P. C. (2016). Body ram, not suction, is the primary axis of suction-feeding diversity in spiny-rayed fishes. *Journal of Experimental Biology* **219**, 119-128.

McClenahan, P., Troup, M. and Scott, E. K. (2012). Fin-tail coordination during escape and predatory behavior in larval zebrafish. *PloS One* **7**, e32295.

McKinnon, A.D., Duggan, S., Nichols, P.D., Rimmer, M.A., Semmens, G. and Robino, B. (2003). The potential of tropical paracalanid copepods as live feeds in aquaculture. *Aquaculture* **223**, 89-106.

Østergaard, P., Munk, P. and Janekarn, V. (2005). Contrasting feeding patterns among species of fish larvae from the tropical Andaman Sea. *Marine Biology* **146**, 595-606.

R Development Core Team (2017). R: A language and environment for statistical computing. In *R Foundation for Statistical Computing*, vol. 2018. Vienna, Austria.

Robinson, H. E., Strickler, J. R., Henderson, M. J., Hartline, D. K. and Lenz, P. H. (2019). Predation strategies of larval fish capturing evasive copepod prey. *Marine Ecology Progress Series*. in press.

Rosenthal, H. (1969). Untersuchungen über das Beutefangverhalten bei Larven des Herings *Clupea harengus*. *Marine Biology* **3**, 208-221.

Rosenthal, H. and Hempel, G. (1970). Experimental studies in feeding and food requirements of herring larvae (*Clupea harengus* L.). In *Marine Food Chains*, (ed. J. H. Steele), pp. 344-364. Berkeley and Los Angeles: University of California Press.

Schindelin, J., Arganda-Carreras, I., Frise, E., Kaynig, V., Longair, M., Pietzsch, T., Preibisch, S., Rueden, C., Saalfeld, S., Schmid, B. et al. (2012). Fiji: an open-source platform for biological-image analysis. *Nature Methods* **9**, 676-682.

Tuttle, L. J., Robinson, H. E., Takagi, D., Strickler, J. R., Lenz, P. H. and Hartline, D. K. (2019). Going with the flow: hydrodynamic cues trigger directed escapes from a stalking predator. *Journal of the Royal Society Interface*, **16**, 20180776.

Voesenek, C. J., Muijres, F. T. and van Leeuwen, J. L. (2018). Biomechanics of swimming in developing larval fish. *Journal of Experimental Biology* **221**, jeb149583.

von Herbing, I. H. and Gallager, S. M. (2000). Foraging behavior in early Atlantic cod larvae (*Gadus morhua*) feeding on a protozoan (*Balanion* sp.) and a copepod nauplius (*Pseudodiaptomus* sp.). *Marine Biology* **136**, 591-602.

Webb, P. W. and Skadsen, J. M. (1980). Strike tactics of *Esox*. *Canadian journal of zoology* **58**, 1462-1469.

Wittenrich, M. L. and Turingan, R. G. (2011). Linking functional morphology and feeding performance in larvae of two coral-reef fishes. *Environmental Biology of Fishes* **92**, 295-312.

Figures

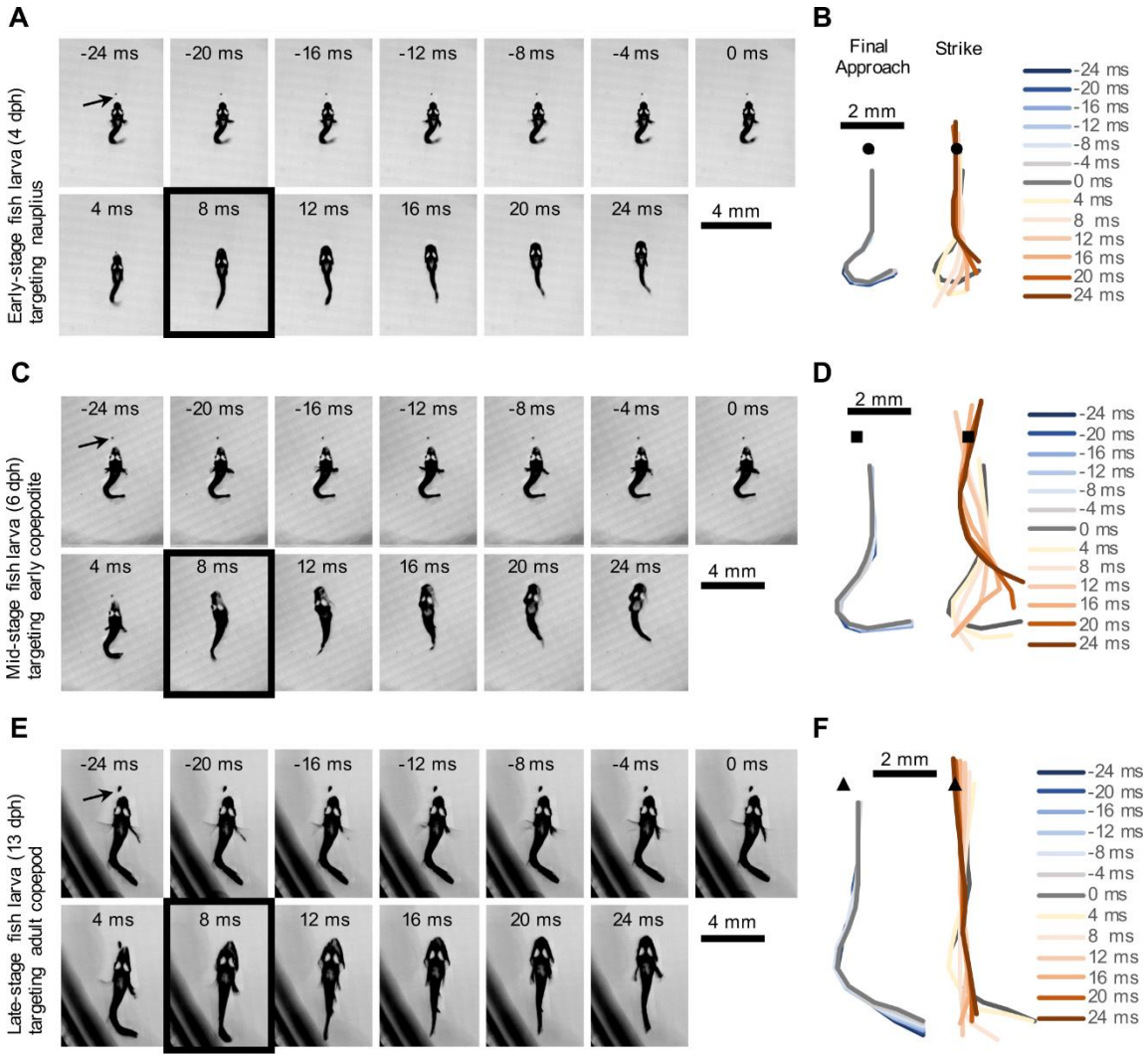

Fig. 1. Exemplar feeding sequences of larval clownfish in 4-ms intervals (every other frame at 500 fps). Frames in (A), (C), and (E) show the position of the fish during the approach, at t_0, and during the propulsive strike and recovery. The black arrow points to the copepod and the black box surrounds the time at which the copepod was engulfed. (B), (D), and (F) show the midlines of the fish shown in (A), (C), and (E), respectively. The left lines represent the fish's midline during the final approach (t_{-24} to t_0). The right lines represent the fish's midline through the strike (t_0 to t_{+24}). The position of the nauplius, copepodite, and adult copepod are indicated with a circle, square, and triangle respectively. Unique scales provided for each section, A-F.

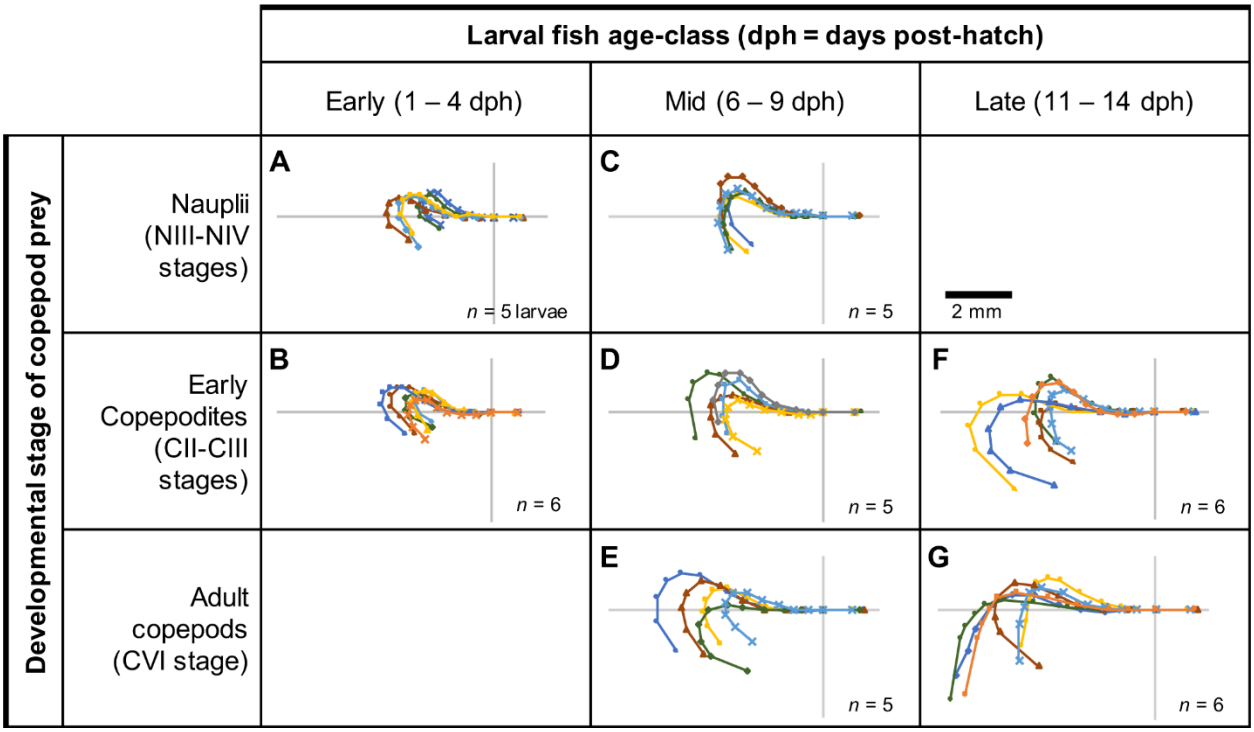

Fig. 2. Postures of larval clownfish just before successful strikes. Each line represents an individual larva's midline at t_0, grouped by predator-prey category (n = 7 categories based on larval age-class and copepod developmental stage, with sample sizes within each group shown in A-G). The x,y origin for each individual is a pigment spot between its eyes. The point representing the leading edge of a fish's mouth extends to the right, along the x-axis. Postures have been rotated and flipped to show curvature in the same direction, for ease of comparison. The scale bar is shown in the top right, and is the same for all plots within the figure.

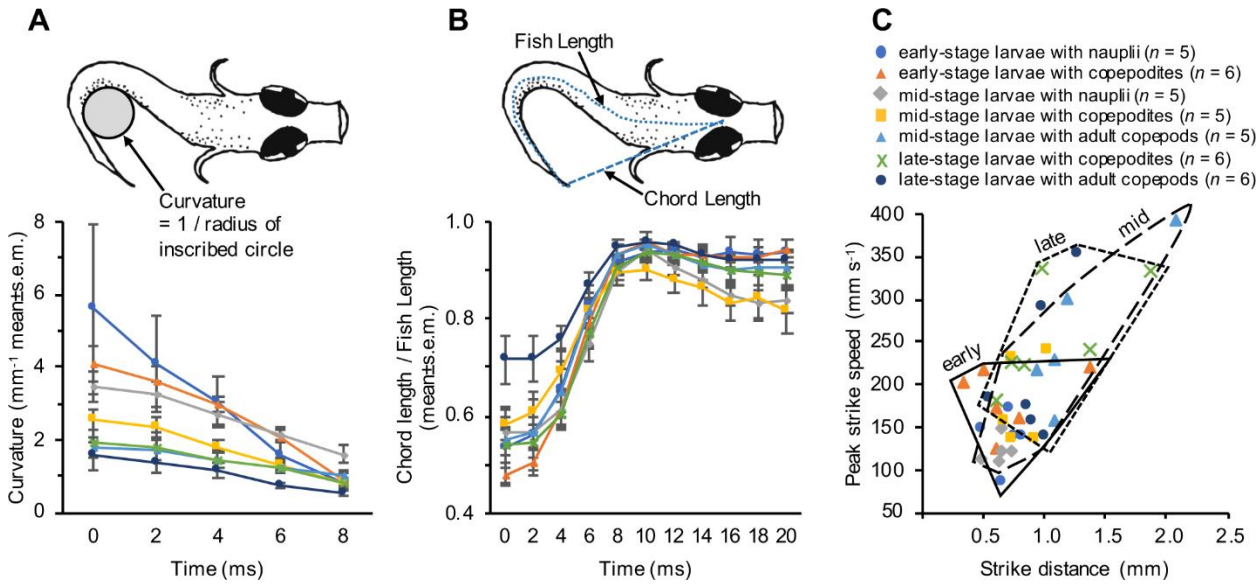

Fig. 3. Fish larvae's relative curvature (A, B) and performance as a function of strike distance (C), shown by predator-prey category (*n* = 7 categories based on larval age-class and copepod developmental stage). (A) Curvature derived from the reciprocal radius of a circle inscribed within the tail of each fish, as shown in drawing, and averaged within predator-prey category during the initial lunge. (B) Curvature normalized by dividing the chord length by the fish length for each fish, as shown in drawing, and averaging within predator-prey category. (C) Peak velocity during each larva's strike, plotted vs. distance between the edge of the fish's mouth and the rostrum of the copepod at t_0 (i.e., strike distance). Polygons enclose individual points by larval age-class. Sample sizes indicated in (C).

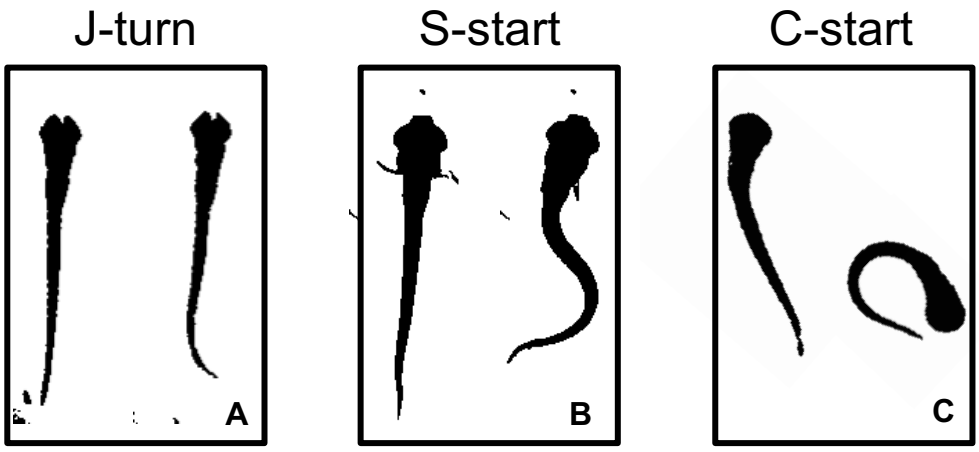

Fig. S1. Examples of postures in larval zebrafish associated with a J-turn (A), a predatory S-start (B) and an escape C-start (C). (A) Zebrafish larva at 7 days post-fertilization (dpf, 1st feeding at 5 dpf) approaching a *Paramecium* prey (left, *t*=0.140 s) and the same larva during a J-turn (right, *t*=0.217 s), which serves to slightly reorient the larva toward its prey. (B) Zebrafish at 5 dpf setting up for an S-start (left, *t*=-0.008 s) and in the S-start posture (right, *t*=-0.003 s), both prior to mouth opening (*t*=0) and strike. (C) Zebrafish at 7 dpf swimming (left, *t*=0.012 s) and in the C-bend (right, *t*=0.022 s) prior to the fast-start escape (*t*~0.026 s). Images were modified from examples in McClenahan et al. (2012) for (A) and (C), and Voesenek et al. (2018) for (B).

References

McClenahan, P., Troup, M. and Scott, E. K. (2012). Fin-tail coordination during escape and predatory behavior in larval zebrafish. *PloS One* **7**, e32295.

Voesenek, C. J., Muijres, F. T. and van Leeuwen, J. L. (2018). Biomechanics of swimming in developing larval fish. *Journal of Experimental Biology* **221**, jeb149583.

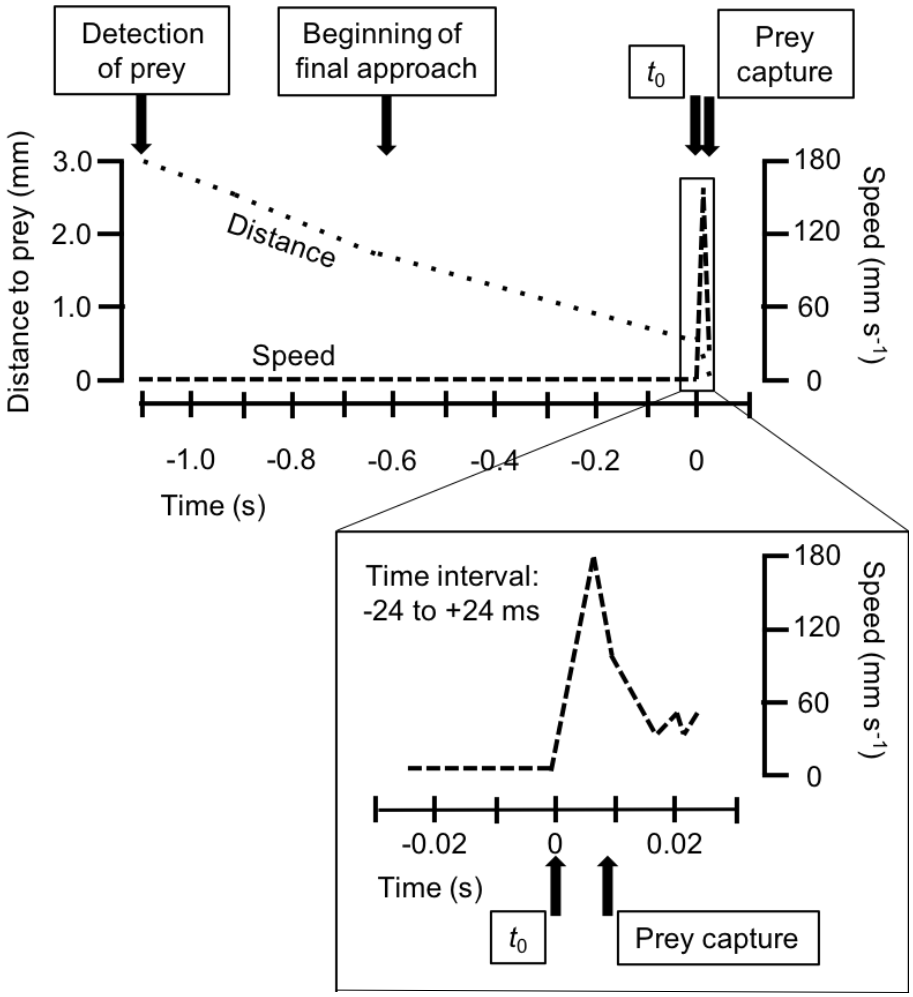

Fig. S2. Schematic diagram of the clownfish larva–copepod interaction starting at detection of prey and continuing through the strike phase, based on Robinson et al. (2019). Times shown for prey detection, the beginning of the final approach phase, t_0, and capture based on observations of an actual predator–prey interaction (Fig. 4 in Robinson et al. 2019) and defined in the Materials and Methods of the current paper. Both distance to prey and swimming speeds of the larval fish are shown as dashed (speed) and dotted (distance) lines. The lower box is an expanded view of the interval analyzed in the current study (-24 to 24 ms) to characterize the strike posture as a function of larval age and copepod stage.

Reference

Robinson, H. E., Strickler, J. R., Henderson, M. J., Hartline, D. K. and Lenz, P. H. (2019). Predation strategies of larval fish capturing evasive copepod prey. *Marine Ecology Progress Series*. in press.

Table S1. Statistical model results.

Results from beta regression and multiple linear regression (MLR) models. Beta regression models were created with the "betareg" function in the *betareg* package in *R*, and MLR models were created with the "lm" function in the standard *stats* package of *R*. Model predictors: *preycat* = categorical variable of the developmental stage of copepod prey (nauplius, copepodite, adult), *dph* = fish's age in days-post-hatch, *preycat:dph* = interaction between preycat and dph, *dph cat* = categorical variable of the age-class of fish (E=early (1-4 dph), M=mid (5-9 dph), L=late (11-14 dph)), and *dist* = distance between the leading edge of the fish's mouth and the copepod rostrum at t_0. Significant p-values ($P < 0.05$) are indicated in **bold**.

Model estimates:
Beta regression: The beta regression uses a logit link, so interpretation of its coefficients is the same as for a log-linear regression. For example, an increase in "X" (continuous predictor) by 1 unit is associated with a multiplicative change of $e^{\text{X Estimate}}$ in the response Y, after accounting for other predictors in the model. For categorical predictors, the comparison is indicated in the "Model predictors" column as "X_1 vs X_2". For instance, late-stage fish larvae that target adult copepods ("A") have a CVF value that is $e^{0.625}$ (=1.87) times that of late-stage larvae that target copepodites ("C"). Greater CVF values indicate lesser curvature (CVF = 1 is a straight/unbent fish).
Multiple linear regression: Because Y (peak strike speed) is logged, an increase of one unit in X (continuous predictor) is associated with a change in the median of Y by a factor of $e^{\text{X Estimate}}$, after accounting for other predictors in the model.

MODEL: Response variable – Dataset, *n*	Model predictors	Estimate	SE	*z* value	*p* value
BETA REGRESSION: Chord length-to-fish length ratio (CVF, ratio) – All fish, *n*=37	Intercept	-0.073	0.175	-0.414	0.679
	preycat, N vs C	0.120	0.289	0.417	0.677
	preycat, A vs C	**-1.176**	**0.550**	**-2.139**	**0.032**
	preycat, A vs N	**-1.297**	**0.570**	**-2.276**	**0.023**
	dph	0.029	0.022	1.291	0.197
	preycat:dph, N vs C	0.004	0.045	0.095	0.924
	preycat:dph, A vs C	**0.154**	**0.056**	**2.744**	**0.006**
	preycat:dph, A vs N	**0.150**	**0.065**	**2.310**	**0.021**
	Log-likelihood: 38.56 on 7 df; Pseudo R-squared: 0.424				
BETA REGRESSION: Chord length-to-fish length ratio (CVF, ratio) – Late-stage fish only, *n*=12	Intercept	-3.350	1.768	-1.894	0.058
	preycat, A vs C	**0.625**	**0.213**	**2.931**	**0.003**
	dph	**0.305**	**0.153**	**1.987**	**0.047**
	Log-likelihood: 13.6 on 4 df; Pseudo R-squared: 0.627				
MULTIPLE LINEAR REGRESSION: Log(peak strike speed) (mm s^{-1}) – All fish, *n*=37	**Intercept**	**4.560**	**0.117**	**38.85**	**<0.001**
	dist	**0.494**	**0.125**	**3.935**	**<0.001**
	dph cat, M vs E	-0.037	0.102	-0.364	0.718
	dph cat, L vs E	0.077	0.117	0.653	0.518
	preycat, C vs N	**0.304**	**0.104**	**2.915**	**0.006**
	preycat, A vs N	**0.292**	**0.129**	**2.255**	**0.031**
	preycat, A vs C	-0.012	0.102	-0.114	0.91
	Residual SE: 0.241 on 24 df; Adjusted R-squared: 0.539; $F_{5,32}$ = 9.65; p<0.001				

Movie 1. Representative examples of *A. ocellaris* clownfish larvae striking at *B. similis* copepods. Clownfish are identified as early-stage (1-4 days post-hatch, dph), mid-stage (6-9 dph), or late-stage (11-14 dph). Copepods are identified as a nauplius (NIII-NIV stages), copepodite (CII-CIII stages), or adult (CVI stage). Video is slowed down to one-tenth speed (50 frames per second, fps) and a scale bar is present in the bottom left of each clip.

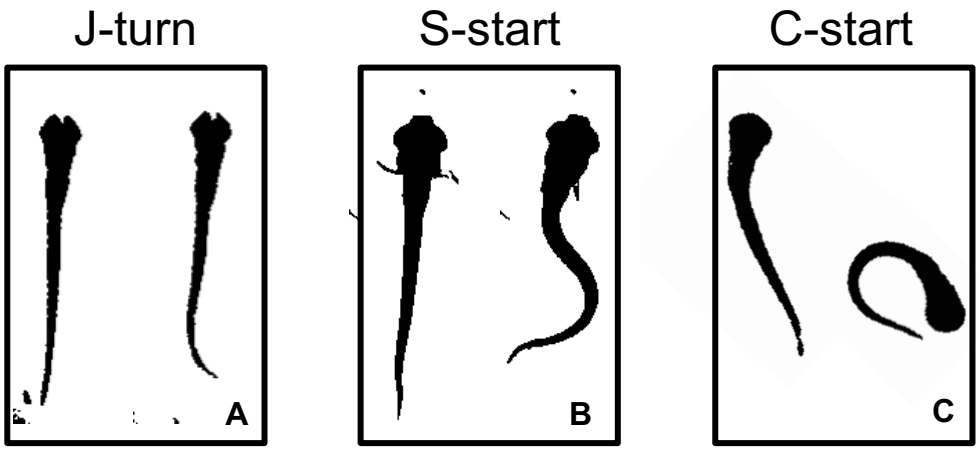

Fig. S1. Examples of postures in larval zebrafish associated with a J-turn (A), a predatory S-start (B) and an escape C-start (C). (A) Zebrafish larva at 7 days post-fertilization (dpf, 1st feeding at 5 dpf) approaching a *Paramecium* prey (left, *t*=0.140 s) and the same larva during a J-turn (right, *t*=0.217 s), which serves to slightly reorient the larva toward its prey. (B) Zebrafish at 5 dpf setting up for an S-start (left, *t*=-0.008 s) and in the S-start posture (right, *t*=-0.003 s), both prior to mouth opening (*t*=0) and strike. (C) Zebrafish at 7 dpf swimming (left, *t*=0.012 s) and in the C-bend (right, *t*=0.022 s) prior to the fast-start escape (*t*~0.026 s). Images were modified from examples in McClenahan et al. (2012) for (A) and (C), and Voesenek et al. (2018) for (B).

References

McClenahan, P., Troup, M. and Scott, E. K. (2012). Fin-tail coordination during escape and predatory behavior in larval zebrafish. *PloS One* **7**, e32295.

Voesenek, C. J., Muijres, F. T. and van Leeuwen, J. L. (2018). Biomechanics of swimming in developing larval fish. *Journal of Experimental Biology* **221**, jeb149583.

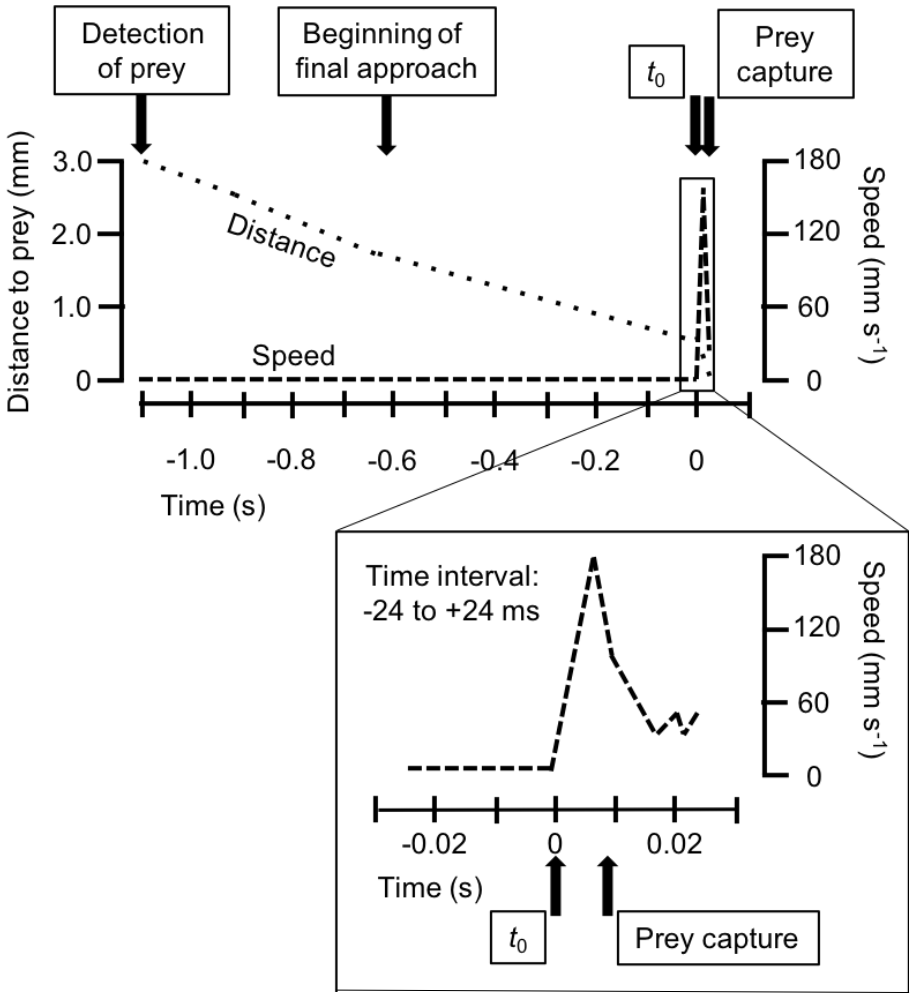

Fig. S2. Schematic diagram of the clownfish larva–copepod interaction starting at detection of prey and continuing through the strike phase, based on Robinson et al. (2019). Times shown for prey detection, the beginning of the final approach phase, t_0, and capture based on observations of an actual predator–prey interaction (Fig. 4 in Robinson et al. 2019) and defined in the Materials and Methods of the current paper. Both distance to prey and swimming speeds of the larval fish are shown as dashed (speed) and dotted (distance) lines. The lower box is an expanded view of the interval analyzed in the current study (-24 to 24 ms) to characterize the strike posture as a function of larval age and copepod stage.

Reference

Robinson, H. E., Strickler, J. R., Henderson, M. J., Hartline, D. K. and Lenz, P. H. (2019). Predation strategies of larval fish capturing evasive copepod prey. *Marine Ecology Progress Series*. in press.

Table S1. Statistical model results.

Results from beta regression and multiple linear regression (MLR) models. Beta regression models were created with the "betareg" function in the *betareg* package in *R*, and MLR models were created with the "lm" function in the standard *stats* package of *R*. Model predictors: *preycat* = categorical variable of the developmental stage of copepod prey (nauplius, copepodite, adult), *dph* = fish's age in days-post-hatch, *preycat:dph* = interaction between preycat and dph, *dph cat* = categorical variable of the age-class of fish (E=early (1-4 dph), M=mid (5-9 dph), L=late (11-14 dph)), and *dist* = distance between the leading edge of the fish's mouth and the copepod rostrum at t_0. Significant p-values ($P < 0.05$) are indicated in **bold**.

Model estimates:
Beta regression: The beta regression uses a logit link, so interpretation of its coefficients is the same as for a log-linear regression. For example, an increase in "X" (continuous predictor) by 1 unit is associated with a multiplicative change of $e^{\text{X Estimate}}$ in the response Y, after accounting for other predictors in the model. For categorical predictors, the comparison is indicated in the "Model predictors" column as "X_1 vs X_2". For instance, late-stage fish larvae that target adult copepods ("A") have a CVF value that is $e^{0.625}$ (=1.87) times that of late-stage larvae that target copepodites ("C"). Greater CVF values indicate lesser curvature (CVF = 1 is a straight/unbent fish).
Multiple linear regression: Because Y (peak strike speed) is logged, an increase of one unit in X (continuous predictor) is associated with a change in the median of Y by a factor of $e^{\text{X Estimate}}$, after accounting for other predictors in the model.

MODEL: Response variable – Dataset, *n*	Model predictors	Estimate	SE	*z* value	*p* value
BETA REGRESSION: Chord length-to-fish length ratio (CVF, ratio) – All fish, *n*=37	Intercept	-0.073	0.175	-0.414	0.679
	preycat, N vs C	0.120	0.289	0.417	0.677
	preycat, A vs C	**-1.176**	**0.550**	**-2.139**	**0.032**
	preycat, A vs N	**-1.297**	**0.570**	**-2.276**	**0.023**
	dph	0.029	0.022	1.291	0.197
	preycat:dph, N vs C	0.004	0.045	0.095	0.924
	preycat:dph, A vs C	**0.154**	**0.056**	**2.744**	**0.006**
	preycat:dph, A vs N	**0.150**	**0.065**	**2.310**	**0.021**
	Log-likelihood: 38.56 on 7 df; Pseudo R-squared: 0.424				
BETA REGRESSION: Chord length-to-fish length ratio (CVF, ratio) – Late-stage fish only, *n*=12	Intercept	-3.350	1.768	-1.894	0.058
	preycat, A vs C	**0.625**	**0.213**	**2.931**	**0.003**
	dph	**0.305**	**0.153**	**1.987**	**0.047**
	Log-likelihood: 13.6 on 4 df; Pseudo R-squared: 0.627				
MULTIPLE LINEAR REGRESSION: Log(peak strike speed) (mm s^{-1}) – All fish, *n*=37	**Intercept**	**4.560**	**0.117**	**38.85**	**<0.001**
	dist	**0.494**	**0.125**	**3.935**	**<0.001**
	dph cat, M vs E	-0.037	0.102	-0.364	0.718
	dph cat, L vs E	0.077	0.117	0.653	0.518
	preycat, C vs N	**0.304**	**0.104**	**2.915**	**0.006**
	preycat, A vs N	**0.292**	**0.129**	**2.255**	**0.031**
	preycat, A vs C	-0.012	0.102	-0.114	0.91
	Residual SE: 0.241 on 24 df; Adjusted R-squared: 0.539; $F_{5,32}$ = 9.65; p<0.001				

Movie 1. Representative examples of *A. ocellaris* clownfish larvae striking at *B. similis* copepods. Clownfish are identified as early-stage (1-4 days post-hatch, dph), mid-stage (6-9 dph), or late-stage (11-14 dph). Copepods are identified as a nauplius (NIII-NIV stages), copepodite (CII-CIII stages), or adult (CVI stage). Video is slowed down to one-tenth speed (50 frames per second, fps) and a scale bar is present in the bottom left of each clip.